AGU ADVANCING EARTH AND SPACE SCIENCES

AGU Advances

RESEARCH ARTICLE
10.1029/2024AV001327

Peer Review The peer review history for this article is available as a PDF in the Supporting Information.

Boreal Forest Fire Causes Daytime Surface Warming During Summer to Exceed Surface Cooling During Winter in North America

M. Helbig[1,2], L. Daw[2], H. Iwata[3,4], L. Rudaitis[2], M. Ueyama[5], and T. Živković[1,6]

[1]GFZ German Research Centre for Geosciences, Potsdam, Germany, [2]Department of Physics and Atmospheric Science, Dalhousie University, Halifax, Nova Scotia, Canada, [3]Department of Environmental Science, Shinshu University, Matsumoto, Japan, [4]Institute for Mountain Science, Shinshu University, Matsumoto, Japan, [5]Graduate School of Agriculture, Osaka Metropolitan University, Sakai, Japan, [6]Department of Biology, Dalhousie University, Halifax, Nova Scotia, Canada

Key Points:

- Wildfire causes summer surface warming to exceed winter surface cooling in the North American boreal forest
- Summer surface warming is mainly caused by reduced efficiency of heat transfer between land and atmosphere
- A strong increase in burned area likely increases the daytime surface warming effect by about a third for the entire Canadian boreal forest

Supporting Information:

Supporting Information may be found in the online version of this article.

Correspondence to:

M. Helbig,
helbig@gfz-potsdam.de

Citation:

Helbig, M., Daw, L., Iwata, H., Rudaitis, L., Ueyama, M., & Živković, T. (2024). Boreal forest fire causes daytime surface warming during summer to exceed surface cooling during winter in North America. *AGU Advances*, *5*, e2024AV001327. https://doi.org/10.1029/2024AV001327

Received 24 MAY 2024
Accepted 15 AUG 2024

Author Contributions:

Conceptualization: M. Helbig
Data curation: M. Helbig, L. Daw, L. Rudaitis
Formal analysis: M. Helbig
Funding acquisition: M. Helbig
Methodology: M. Helbig, H. Iwata, M. Ueyama, T. Živković
Project administration: M. Helbig
Resources: H. Iwata, M. Ueyama
Validation: H. Iwata, M. Ueyama
Visualization: M. Helbig, T. Živković
Writing – original draft: M. Helbig

Abstract Boreal wildfires modify surface climates affecting plant physiology, permafrost thaw, and carbon fluxes. Post-fire temperatures vary over decades because of successional vegetation changes. Yet, the underlying biophysical drivers remain uncertain. Here, we quantify surface climate changes following fire disturbances in the North American boreal forest and identify its dominant biophysical drivers. We analyze multi-year land-atmosphere energy exchange and satellite observations from across North America and find post-fire daytime surface temperatures to be substantially warmer for about five decades while winter temperatures are slightly cooler. Post-fire decadal changes are characterized by decreasing leaf area index during the first decade, by sharply increasing surface albedo during the snow cover period, and by a less efficient heat exchange between the forest and the atmosphere caused by decreasing surface roughness for about 2–3 decades. Over the first three decades, the amount of energy used for evapotranspiration increases before returning to lower values. We find that surface warming is mainly explained by less efficient forest-atmosphere heat exchange while cooling is additionally explained by increasing surface albedo. We estimate that biome-wide daytime surface temperatures of the Canadian boreal forest in 2024 are 0.27°C warmer in the summer and 0.02°C cooler during the winter because of fire. For a scenario with a strong increase in burned area, we estimate annual warming from fire to increase by a third until 2050. Our study highlights the potential for accelerated surface warming in the boreal biome with increasing wildfire activity and disentangles the biophysical drivers of fire-related surface climate impacts.

Plain Language Summary Every year, wildfires in the North American boreal forest burn vast areas, continuously changing the land. Following fires, the surface climate remains impacted for many decades. What causes these slow climatic changes is still debated. Here, we analyze ground observations from fire sites and satellite observations in Canada and the U.S. to better understand the long-lasting consequences of wildfires for the climate in the boreal forest. Following a wildfire, surface daytime temperatures in the summer are warmer for about 50 years while winter surface temperatures are cooler. After a wildfire, the forest is characterized by a reduction in leaves, absorbs less sunlight, and heat is less efficiently transferred from the forest to the atmosphere. Forest water loss to the atmosphere increases for about 30 years before returning to lower levels again. The observed warming is mainly caused by the less efficient heat exchange between the forest and the atmosphere while the winter cooling is caused by increased reflection of sunlight by exposed snow surfaces. With increased wildfire activity, daytime surface temperatures in the Canadian boreal forest are estimated to be up to about 0.4°C warmer in the summer and about 0.2°C annually indicating accelerated surface warming.

1. Introduction

Wildfire represents the most important disturbance agent in the boreal forest (Esseen et al., 1997) and has a pronounced effect on the global carbon budget (Bond-Lamberty et al., 2007; Phillips et al., 2022), the global climate (Randerson et al., 2006), and the regional climate at high latitudes (Ueyama et al., 2020). Covering a surface area of about 1,900 millions of hectares (Brandt et al., 2013), the boreal forest accounts for about half of the global forest area (Keenan et al., 2015). A third of the circumpolar boreal forest is in North America (Brandt et al., 2013), where wildfires burned about 2% (8,740,000 ha) of the forested and wooded area (361,926,000 ha; Brandt, 2009) annually during the period 1959–1999 (Kasischke & Turetsky, 2006). Wildfire is a natural

Writing – review & editing: M. Helbig, L. Daw, H. Iwata, L. Rudaitis, M. Ueyama, T. Živković

disturbance and a crucial component of the life cycle of boreal forest ecosystems contributing to its structural and functional diversity (Esseen et al., 1997). However, in recent decades, fire regimes in the North American boreal forest have changed with exceptionally high fire frequencies leading to increasingly large areas of recently burned boreal forest (Hanes et al., 2019; Kasischke & Turetsky, 2006; Kelly et al., 2013; Veraverbeke et al., 2017). This trend of increasing fire frequency and burned area in the boreal forest is expected to continue and accelerate with ongoing climate change (Balshi et al., 2009). Consequently, the shifting fire regime will alter the structure and composition of vast areas of the boreal forest (Dawe et al., 2022; Stralberg et al., 2018) with potentially large impacts on the regional and global climate (Randerson et al., 2006).

Wildfire impacts on climate can be broadly separated into carbon (C) cycle and biophysical effects (Randerson et al., 2006). For example, during periods of severe and more frequent wildfire activity boreal forests can turn from net C sinks to sources (Harden et al., 2000; Walker et al., 2019) because of enhanced C loss through direct fire CO_2 emissions (Amiro et al., 2001; Walker et al., 2018). Biophysical effects are caused by fire disturbance-induced changes to surface albedo (Betts, 2000), to the partitioning of available energy into sensible heat and into evapotranspiration (i.e., latent heat; Amiro et al., 2006), and to surface roughness (Chambers & Chapin III, 2003). However, how decadal-scale successional changes in the biophysical ecosystem properties affect near-surface climate in the boreal forest remains elusive despite the potential to modify regional climate change trajectories in the boreal biome.

Albedo changes control how much incoming shortwave radiation is absorbed at the land surface and have a direct impact on the Earth's energy budget and, thus, on the global climate (Randerson et al., 2006). In boreal forests, growing season surface albedo has been shown to decrease immediately after fire disturbance (Chambers et al., 2005; Liu et al., 2018; Yoshikawa et al., 2002). With post-fire plant recovery and vegetation growth (Tsuyuzaki et al., 2009), surface albedo slowly increases for about three decades before decreasing to a slightly lower albedo typical of mature boreal forests (Amiro et al., 2006; Liu & Randerson, 2008; Lyons et al., 2008; Potter et al., 2020). The successional albedo dynamics are partly driven by fire severity with high burn severity sites leading to a larger post-fire fraction of deciduous trees and higher growing season albedo compared to low severity burn sites (Beck et al., 2011). During the snow cover period, surface albedo of ecosystems affected by wildfire disturbance has been observed to be higher compared to the pre-fire albedo because of exposure of the highly reflective snow surface (Potter et al., 2020). However, the magnitude of albedo change is variable and depends on fire severity with high fire severity causing larger increases in albedo (Beck et al., 2011; Wang et al., 2016). Additionally, deposition of black carbon (or soot) and burned woody debris from wildfires onto snow surfaces can lead to a temporary reduction in winter albedo lasting for up to a decade (Gleason et al., 2019; Qian et al., 2009).

Changes in energy partitioning affect the amount of evaporative cooling at the land surface (Bonan, 2008), the cooling and moistening of the atmosphere (Ueyama et al., 2020), and the daytime growth of the atmospheric boundary layer (Helbig et al., 2020; Ueyama et al., 2020). Increased fire disturbance in the boreal forest has been shown to decrease regional evapotranspiration compared to pre-fire conditions (Bond-Lamberty et al., 2009; Kang et al., 2006) and reduced evapotranspiration rates compared to mature forests have been observed for several decades after fire disturbance (Barker et al., 2009). However, Liu et al. (2005) only found reduced annual evapotranspiration 3 years after fire disturbance while a 15-year and an 80-year stand experienced similar annual evapotranspiration for a chronosequence study in Alaska. Similarly, Amiro et al. (2006) observed a large increase in Bowen ratio (i.e., ratio of sensible to latent heat exchange between the forest and the atmosphere) immediately after fire disturbance and a wide Bowen ratio range for mature forest sites, which was within the range of a 15-year old burn site in Canada. The large variability in energy partitioning of mature boreal forests highlights the importance of forest type, nutrient status, and soil water status for late post-fire successional stages. Fire-induced changes in evapotranspiration along with altered soil infiltration properties have also direct effects on runoff generation and, thus, can impact downstream water supply (Ebel & Moody, 2017; Hampton & Basu, 2022; Pimentel & Arheimer, 2021).

Post-fire regrowth of vegetation and a more complex canopy structure usually cause an increase in surface roughness (Chambers et al., 2005). The aerodynamically rougher surface leads to enhanced coupling and more efficient heat exchange (i.e., higher aerodynamic conductance) between forest canopy and atmosphere as is typical for mature boreal forests (Baldocchi et al., 2000). More efficient heat exchange helps to minimize the difference between air and canopy temperature, thus, contributing to surface cooling. For example, Panwar

et al. (2020) found aerodynamic conductance to be more important for surface cooling in forests than evaporative effects, which were more important in low stature grasslands. Similarly, Liao et al. (2018) found land surface warming from deforestation to be mainly caused by a reduction in aerodynamic conductance. However, the contribution of changing surface roughness to land surface temperature changes with ongoing post-fire succession remains uncertain.

Several studies have assessed the near-surface climate impacts of wildfire disturbances in the boreal forest. Ueyama et al. (2020) used paired energy balance observations in interior Alaska and an atmospheric mixed layer model to demonstrate an air temperature cooling effect from fire disturbance for at least 13 years after the fire. Similarly, Rogers et al. (2013) found forest composition changes due to wildfire disturbance to cause an air temperature cooling effect across the North American boreal forest using a coupled Earth system model. Other studies have studied wildfire effects on land surface (Chambers & Chapin III, 2003; Liu et al., 2018; Zhao et al., 2021) and soil temperature (Jiang et al., 2015), which is important to understand linkages between fire and permafrost thaw (Gibson et al., 2018; Jiang et al., 2015; Yoshikawa et al., 2002), vegetation heat stress and post-fire vegetation recovery (Nolan et al., 2021), and soil C fluxes (Bronson et al., 2008; Lloyd & Taylor, 1994). In contrast to the reported air temperature cooling effects, for Siberian boreal forests, Liu et al. (2018) found strong warming of summer and weak cooling of winter surface temperatures immediately after fire disturbance with stronger impacts in evergreen than deciduous forests. Based on satellite remote sensing observations, they attributed the warming effect to decreasing evapotranspiration. Using satellite observations over the North American boreal forest, Zhao et al. (2021) identified a similar strong daytime surface warming and a weak daytime cooling effect from wildfires during the summer and winter, respectively. The magnitude of the surface temperature change depended on fire severity. Summer warming was mostly driven by reduced evapotranspiration while winter cooling was mostly driven by increasing post-fire surface albedo. In a global forest fire study, Liu et al. (2019) found similar land surface temperature effects across the circumpolar boreal forest. However, they found the annual post-fire warming to only last for about 5 years before an albedo-induced cooling effect was observed in years six to nine after fire disturbance. The discrepancies between reported fire-induced warming and cooling effects highlight the complexity of land surface and air temperature changes and their underlying biophysical drivers. While these studies shed light on fire disturbance effects on land surface and air temperatures within a few years after disturbance, comprehensive studies on multi-decadal post-fire successional changes are lacking.

Understanding land surface temperature dynamics and its drivers during all post-fire successional stages is crucial to better understand recent and future land surface temperature trends in the boreal forest. With changing fire regimes (Kelly et al., 2013), boreal forest composition and structure is shifting and is expected to further change with ongoing climate change (Beck et al., 2011; de Groot et al., 2013) potentially modifying climate change trajectories. Here, we study North American boreal forest land surface temperature dynamics over multi-decadal successional post-fire stages and their potential biophysical drivers (i.e., changes in efficiency of heat exchange between the forest and the atmosphere, albedo, and energy partitioning). Using satellite observations, we first assess how time since wildfire disturbance affects recent land surface temperature, surface albedo, and leaf area index (LAI) dynamics across 142 sites in the Canadian and Alaskan boreal forest. Using in situ eddy covariance flux tower observations from a chronosequence of 13 sites in Canada and Alaska, we then assess how post-fire albedo, energy partitioning, and aerodynamic conductance (i.e., efficiency of heat exchange between the forest and the atmosphere) contribute to the observed land surface temperature changes across different post-fire successional stages. Finally, we use historical and projected changes in burned area in the Canadian boreal forest and satellite-derived trajectories of post-fire land surface temperature to quantify current and potential future impacts of wildfire disturbance on land surface temperatures of the boreal forest.

2. Materials and Methods

2.1. Data

2.1.1. Satellite Observations From MODIS Terra and Aqua

To assess trajectories of post-fire daytime land surface temperatures, we used 8-day, quality controlled, composite land surface temperature from the MODIS Aqua MYD21A2 and Terra MOD21A2 products (Hulley, 2021; Hulley & Hook, 2017). The spatial resolution of both products is 1 km^2. Observations are for 10:30hr local time (for Terra) and 13:30hr local time (for Aqua). Across the Canadian and Alaskan boreal forest (delineated

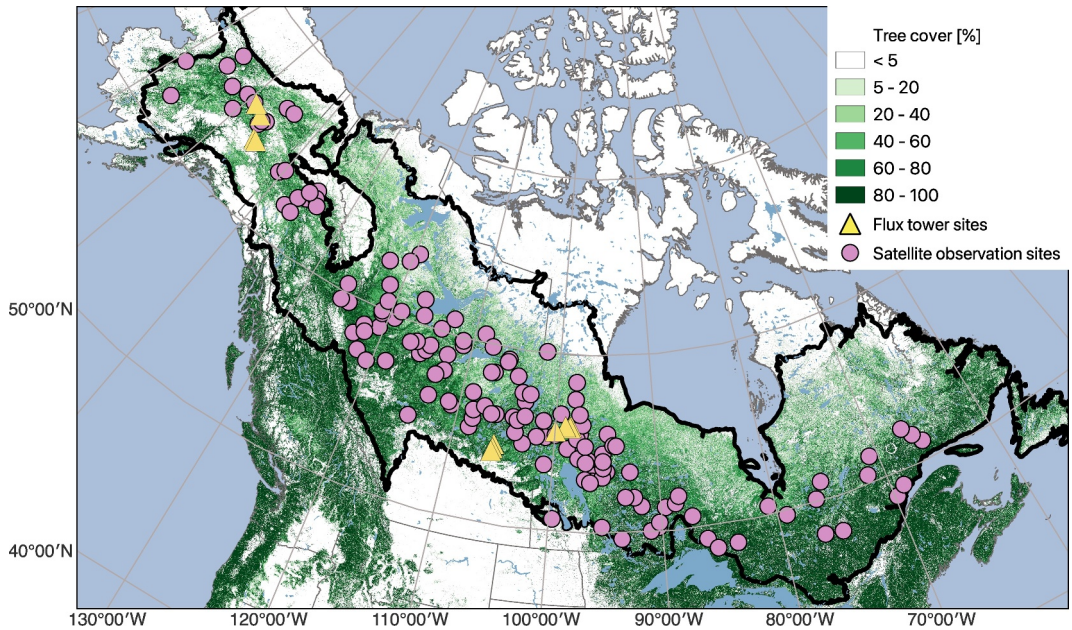

Figure 1. Map of the North American boreal biome and location of eddy covariance flux tower (triangles) and satellite remote sensing (circles) study sites. Green shading indicates tree cover percentage from Hansen et al. (2013). Black solid line shows the boundary of the boreal biome.

according to Brandt (2009)), 142 sites of different fire disturbance age were selected covering a wide range of successional regrowth stages (Figure 1). Fire information across the entire extent of the boreal forest in Canada and Alaska was taken from the Canadian National Fire Database (CNFD) and the Wildland Fire Decision Support System (WFDSS) Interagency Fire Perimeter History data set, respectively. For each site, the year of fire and the size of the fire were recorded, and satellite time series were extracted using the Global Subsets Tool provided by ORNL DAAC (ORNL DAAC, 2018). Median fire perimeter size was 26,169 ha ranging from a minimum of 926 ha to a maximum size of 596,459 ha. Median year of fire disturbance was 1981 ranging from 2014 to 1928. Each site was paired with a nearby control site outside of the fire perimeter. Median distance between fire and control site was 8.7 km with a minimum of 2.4 km and a maximum of 37.7 km (Table S1 in Supporting Information S1). Control sites were outside of historical fire perimeters as verified based on the CNFD and WFDSS data sets. Land cover composition of each selected MODIS pixel was extracted from the 30 m 2020 Land Cover of Canada (Natural Resources Canada, 2020) and from the 30 m Alaska National Land Cover Database 2016 (USGS, 2016). On average, 1 km pixels at fire sites comprised 41% evergreen needleleaf forests, 29% shrublands, 15% wetlands, and 14% deciduous broadleaf and mixed forests. Control sites comprised 69% evergreen needleleaf forests, 8% shrublands, 11% wetlands, and 9% deciduous broadleaf and mixed forests. With time since fire disturbance, evergreen needleleaf forest cover increased and shrubland cover decreased at the fire sites (Figure S1 in Supporting Information S1).

For the same sites, we additionally extracted time series of 8-day composite LAI based on the MODIS Terra MOD15A2H product (Myneni et al., 2015) and of daily shortwave white-sky albedo based on the MODIS Terra + Aqua MCD43A product (Schaaf & Wang, 2021). Time series from MODIS Aqua covered the period 2002–2022 and from MODIS Terra the period 2000–2022.

2.1.2. Eddy Covariance Flux Tower Observations

In this study, we analyze land-atmosphere energy fluxes and meteorological observations from 13 eddy covariance flux tower sites in the North American boreal forest characterized by a range of wildfire histories (Figure 1 and Table S2 in Supporting Information S1). Flux tower data sets were retrieved from the AmeriFlux database (https://ameriflux.lbl.gov/) using the *amerifluxr* package (Chu & Hufkens, 2022) in the R environment (R version 4.1.2). Only sites with a documented history of wildfire disturbance within 80 years prior to measurements were selected. In total, we analyzed 53 site-years ranging from 2 to 75 years after fire disturbance.

2.2. Methods

2.2.1. Satellite Time Series Analysis

Time series of daily differences in daytime land surface temperature, surface albedo, and leaf area index (LAI) between burn and control sites were extracted for each site pair to analyze seasonal changes in fire impacts. For LAI, we compared growing season LAI differences only (defined as July–September). Differences were then averaged by decade after fire disturbance for each day of year. Additionally, differences were averaged for all years before fire disturbance.

2.2.2. Analysis of Land-Atmosphere Flux and Meteorological Observations

To assess the ability of the ecosystems to cool the land surface, we analyzed the difference between daily afternoon (12:00–16:00 hr local time) air and land surface temperature [ΔT, °C] (e.g., Panwar et al., 2020). We chose this approach since there were no control sites for the flux tower observations. We focused on afternoon conditions when surface temperatures usually reach their daily maximum since peak temperatures are most relevant when assessing heat stress or permafrost thaw impacts. Here, we use the aerodynamic temperature (i.e., temperature at the height of the roughness length of heat) as a proxy for land surface temperature since direct observations of canopy temperature were only available for some sites. It should be noted that the aerodynamic temperature differs to varying degrees from the radiometric surface temperature as sensed by satellites (Mahrt et al., 1997). To account for different air temperature measurement heights, we extrapolated air temperature measurements for each site to 10 m above the zero plane displacement height (using Equation 4 in Novick and Katul (2020)).

To analyze seasonal dynamics, we analyzed late winter (February–April) and late summer (July–September) observations separately. Late winter was defined as the last 3 months before average snowmelt in the North American boreal forest ends (May 10th with 5th and 95th percentile being April 15th and June 5th, respectively, derived from O'Leary III et al. (2020)). The late growing season between July and September was chosen to ensure that the canopy has fully developed at the sites and that snowmelt is completed. For each season, year, and site, we derived mean daily differences between afternoon surface and air temperature. As potential drivers of post-fire surface climate, we assessed evaporative cooling, efficiency of heat exchange between the land and the atmosphere, and available energy. We used evaporative fraction (i.e., land-atmosphere latent heat flux divided by the sum of land-atmosphere sensible and latent heat flux), bulk aerodynamic conductance [G_a, mm s^{-1}], and surface albedo as explanatory variables. Aerodynamic conductance was derived from measurements of wind speed and friction velocity, as implemented in the *aerodynamic.conductance* function in the *bigleaf* R package (Knauer et al., 2022) where the excess resistance of heat transfer is calculated after Thom (1972). Albedo was calculated as the ratio of outgoing shortwave radiation and incoming shortwave radiation measured at the flux tower locations.

We plotted average ΔT, evaporative fraction, G_a, and albedo for each tower site against years since fire to track post-fire successional changes in ecosystem properties. Then, we fitted asymptotic regression models to the data where applicable. We used the *nls* function with initial parameters estimated with the *SSasymp* self-starting function from the *stats* R package. To assess the drivers of ΔT during post-fire succession, we partitioned the variation in ΔT explained by G_a and albedo for late winter and evaporative fraction, G_a, and albedo for late summer using partial regression as implemented in the *varpart* function of the *vegan* R package (Oksanen et al., 2024). We did not include evaporative fraction as an explanatory variable for late winter since evapotranspiration is small and sensible heat flux is often negative during the snow-covered period. To avoid bias in the partitioning results due to unequal time series lengths between sites, we randomly selected 1 year per site and applied the variation partitioning to the subset of the data. This procedure was repeated 1,000 times before extracting the median, and the 5th and 95th percentile of the explained variation.

2.2.3. Estimating Wildfire Impact on Current and Future Boreal Land Surface Temperatures

To estimate the first-order impact of wildfires on land surface temperatures in the boreal biome, we combined the satellite-derived (daytime) land surface temperature differences between fire and control sites with both historical estimates of burned area and projections of future changes to burned area in the boreal biome. Here, we analyze impacts on surface temperatures only for the boreal biome in Canada due to the availability of historical burned

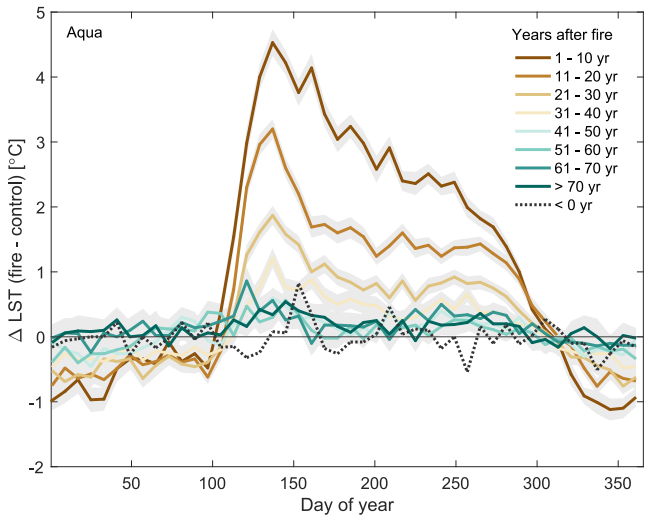

Figure 2. Mean land surface temperature differences (ΔLST) derived from NASA's Aqua satellite between fire disturbance and control sites before (dashed line) and after the fire disturbance (solid lines for individual post-fire decades). Shaded area indicates standard error. Satellite observations are for 142 sites for the period 2002–2022. Observations are for 13:30hr local time. Time since fire disturbance was determined based on the Canadian National Fire Database (CNFD) and the Wildland Fire Decision Support System (WFDSS) Interagency Fire Perimeter History data set.

area products for this region. First, we extracted the annual burned area from the Natural Resources Canada Burned Area Composite data set (https://cwfis.cfs.nrcan.gc.ca/datamart/metadata/nbac) for the years 1986–2023. Burned area was clipped to a boreal biome map for Canada (Brandt, 2009). Second, we derived the land surface temperature effect of wildfire as a function of years since fire from the satellite-derived land surface temperature data. The analysis was conducted for the entire year, to differentiate between winter and summer effects. Third, we weighted the fire impacts using the fraction of adjusted burned area (Skakun et al., 2021) per year relative to the entire surface area of the Canadian boreal biome (including water bodies). Lastly, we summed up the annual effects to estimate the cumulative fire impact on land surface temperatures for the year 2024 (i.e., how much warmer or colder would the Canadian boreal biome be without fire). Here, we assume that the fire effect for years before 1986 is negligible (i.e., 37 years after fire). We also did not account for the immediate impact on land surface temperature for the year of fire. In addition to annual effects, we estimated temperature effects for late summer and winter as defined above. To estimate future fire impacts on land surface temperatures, we used estimated changes in burned area for the Canadian boreal forest between 2020 and 2050 (Phillips et al., 2022). Phillips et al. (2022) report an estimated increase between 36% and 150%, which was used as a low and high burned area increase scenario, respectively (calculated relative to the mean burned area between 2011 and 2020). We then repeated the procedure outlined above to update fire impacts on surface temperatures for the years 2024–2050 for the low and high burned area increase scenarios.

3. Results

3.1. Successional Changes in Land Surface Temperature, Leaf Area Index, and Albedo

Afternoon (13:30hr local time) land surface temperatures increased during the snow-free season by up to 4.7°C in the first decade after the fire disturbance in mid-May before the warming effect decreased to 1.0°C in October (Figure 2). Peak warming decreased with time after fire disturbance and dropped below 1.0°C in the fifth post-fire decade. In contrast, wintertime temperatures of fire sites were cooler during the first few post-fire decades between mid-November and April. However, the cooling effect remained small with generally less than 1°C of cooling. Late morning (10:30hr local time) temperature differences showed similar warming and cooling patterns (see Figure S2 in Supporting Information S1).

Leaf area index decreased by about 50% in the first year after the fire disturbance. Regrowth during the successional stages caused leaf area index to reach pre-fire levels about 10 years post-fire (Figure 3). Continued vegetation growth then led to leaf area index exceeding pre-fire levels between about 40 and 60 years after the fire disturbance. Similarly, Bond-Lamberty et al. (2002) found LAI across a fire chronosequence in Manitoba, Canada, to peak at a 71-year stand before returning to smaller LAI at a 131-year stand.

Albedo differences were largest in February and March during the second decade after the fire disturbance with disturbance sites featuring an albedo that is >0.15 larger than that of the control sites (Figure 4). With snowmelt, the differences rapidly reduced to ~0.02 between May and October. Differences in the first decade after the fire were about 0.14 and 0.01 in February and March and May–October, respectively. Soot deposition and burned woody debris has been shown before to lower snow albedo during the winter within the first post-fire decade (Gleason et al., 2019). Only in the fifth decade after the fire, albedo differences fell below 0.05 during the winter and below 0.01 in the summer.

At the eddy covariance flux tower sites, successional trajectories of differences between aerodynamic and air temperatures (ΔT) showed opposing trends during the late winter and the late summer (Figure 5). During the winter, ΔT increased over time after the fire disturbance while, during the summer, ΔT decreased during the first few decades after the fire disturbance. The post-fire warming effect in the summer was larger in magnitude but asymptotic conditions were reached earlier than for the post-fire cooling effect in the winter. ΔT was significantly

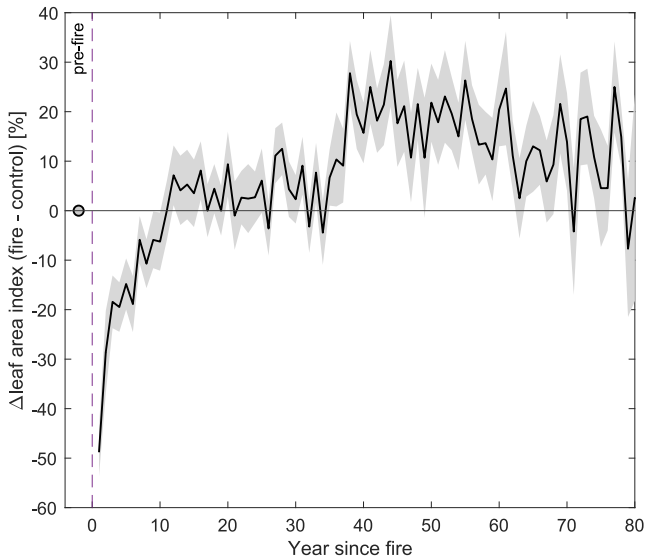

Figure 3. Median difference in leaf area index (July–September) derived from NASA's Aqua satellite between fire disturbance and control sites before and after the fire disturbance (n = 142). Gray shaded area shows standard error. Satellite observations are for the period 2002–2022. Time since fire disturbance was determined based on the Canadian National Fire Database (CNFD) and the Wildland Fire Decision Support System (WFDSS) Interagency Fire Perimeter History data set.

correlated with the difference between satellite-derived land surface temperature (ΔLST) at the fire-affected eddy covariance flux tower sites and nearby control sites. ΔT explained 44% and 62% of the variance in ΔLST in late winter and summer, respectively (see Figure S3 in Supporting Information S1).

Successional changes in surface albedo (Figure 6) were most pronounced during the winter when the ground is snow covered with albedo dropping from about 0.7 to below 0.2 within the first few decades after the fire disturbance. Some sites were characterized by standing burned trees and substantially lower albedo within the first decade after the fire disturbance (<0.45). As indicated above, the lower albedo could also be caused by soot deposition or burned woody debris "darkening" the snow surface at these sites. Decreasing albedo was also observed with ongoing succession during the summer. However, the decrease was less than 0.05 during the 80 years after the fire disturbance with surface albedo being below 0.2 for the entire observation period.

Afternoon aerodynamic conductance for heat increased from 0.02 to about 0.05 m s^{-1} during the first five decades at most sites (Figure 7) except for the sites that featured standing burned trees in the first decade after the fire (Figure S4 in Supporting Information S1, e.g. CA-NS7, CA-SF3). Sites with standing dead trees featured the largest aerodynamic conductance (>0.05 m s^{-1}). The sites with standing burned trees also show lower winter surface albedo compared to other sites of the same post-fire age (see Figure 6).

The fraction of available energy at the land surface that is partitioned to evapotranspiration (i.e., evaporative fraction) during the summer (Figure 8) increased during the first three decades from about 0.4 to about 0.6 before returning to about 0.4 after 40 years after the fire disturbance. For the studied sites, black spruce started to dominate over jack pine after about 40 years (Table S2 in Supporting Information S1). Interannual variability at

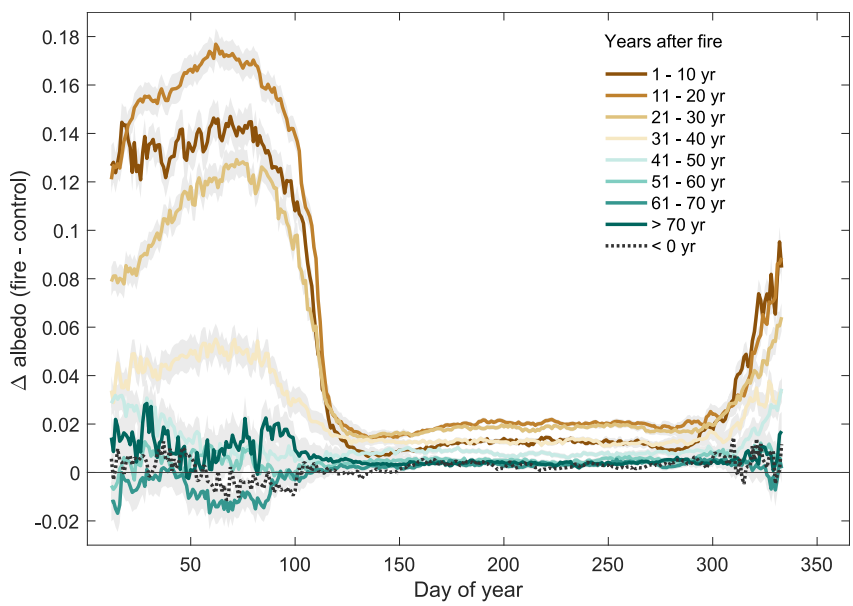

Figure 4. Average daily differences in satellite-derived white-sky surface albedo (MCD43A) between fire disturbance and control sites (n = 142) for eight decades after the fire disturbance (solid lines) and before the fire disturbance (dotted line). Gray shaded areas indicate standard errors. Satellite observations are for the period 2000–2022. Time since fire disturbance was determined based on the Canadian National Fire Database (CNFD) and the Wildland Fire Decision Support System (WFDSS) Interagency Fire Perimeter History data set.

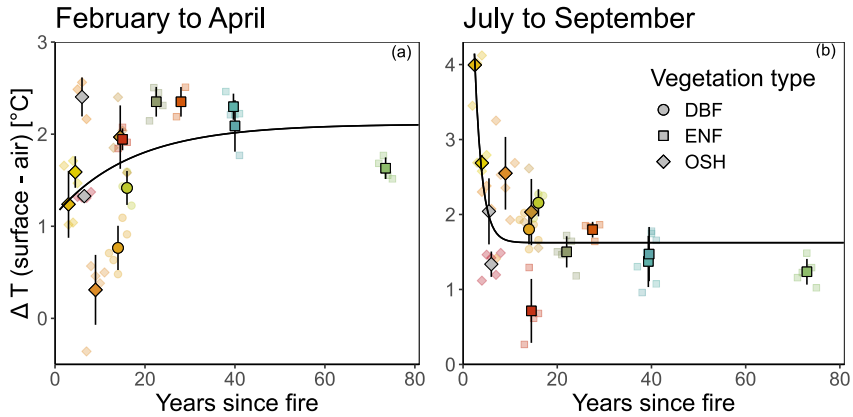

Figure 5. Successional trajectories of differences between afternoon aerodynamic surface and air temperatures for late winter (a) and late summer (b). Solid circles show mean site averages. Symbols indicate vegetation type (DBF = deciduous broadleaf forest, ENF = evergreen needleleaf forest, OSH = open shrubland). Light colored circles show individual years. Solid lines show asymptotic regression fits to site averages. Gray colored symbols show sites with dominance of standing dead trees.

individual sites was large but of smaller magnitude compared to the successional changes and most likely driven by interannual differences in water availability and meteorological conditions.

Winter- and summertime surface-to-air temperature differences across post-fire successional stages were driven by differing drivers. During the summer, aerodynamic conductance, evaporative fraction, and albedo explained together 64% ± 3% of the variance in ΔT with most of the variance being uniquely explained by aerodynamic conductance (34% ± 9%) (Figure 9). In the winter, aerodynamic conductance and albedo together explained 29% ± 6% of the variance in ΔT. However, ΔT differences between successional stages were mainly explained jointly by albedo and aerodynamic conductance (21% ± 6%) while 0% and 7% were uniquely explained by albedo and aerodynamic conductance, respectively. The strong joint effect is likely caused by the winter dependence of both albedo and aerodynamic conductance on canopy height and forest stand complexity, which increases with time since fire disturbance (Cho et al., 2011; Halim et al., 2019). Evaporative fraction was not analyzed as a driver during the winter because of the low evaporation rates during this season. When analyzing the relationship between satellite-derived ΔLST and surface albedo and LAI, we find that 53% and 73% of the variation in temperature difference averaged by year after fire was explained in the late winter and late summer, respectively (Figure S5 in Supporting Information S1). During the winter, albedo explained uniquely 43% of the variation in temperature differences, while LAI explained uniquely 66% during the summer. Leaf area index can both control

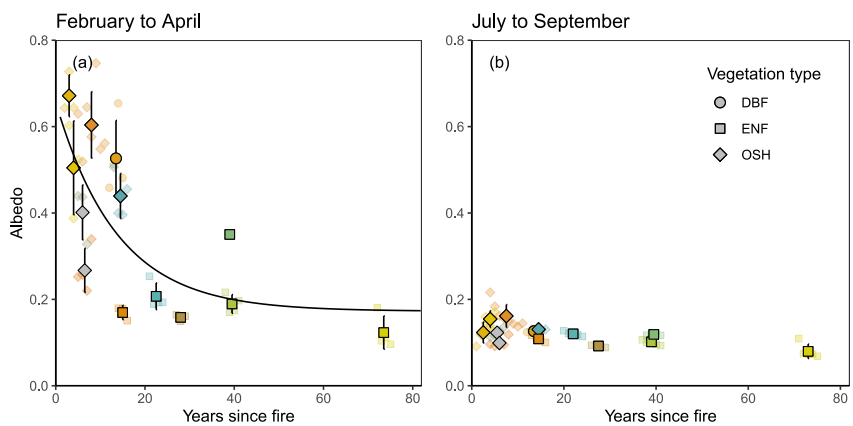

Figure 6. Successional trajectories of surface albedo measured at the flux tower sites for late winter (a) and late summer (b). Solid circles show mean site averages. Symbols indicate vegetation type (DBF = deciduous broadleaf forest, ENF = evergreen needleleaf forest, OSH = open shrubland). Light colored circles show individual years. Solid lines show asymptotic regression fits to site averages. Gray colored symbols show sites with dominance of standing dead trees.

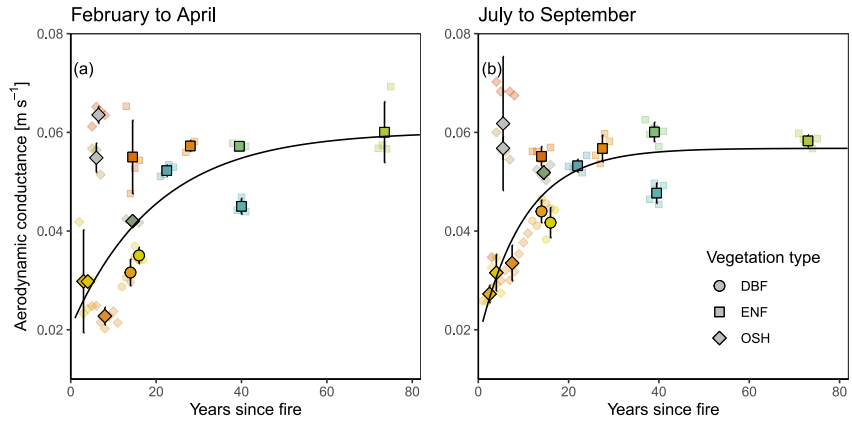

Figure 7. Successional trajectories of mean afternoon aerodynamic conductance for heat for late winter (a) and late summer (b). Solid circles show mean site averages. Symbols indicate vegetation type (DBF = deciduous broadleaf forest, ENF = evergreen needleleaf forest, OSH = open shrubland). Gray colored symbols show sites with dominance of standing dead trees. Light colored circles show individual years. Solid lines show asymptotic regression fits to site averages (excluding sites with standing dead trees).

aerodynamic conductance and evapotranspiration through its effect on vegetation roughness and surface conductance, respectively (Leuning et al., 2008; Lindroth, 1993; Nakai et al., 2008).

3.2. Wildfire Impacts on the Land Surface Temperature of the Boreal Biome

Our study revealed that wildfire in the North American boreal biome cools daytime land surface temperatures in the winter and warms daytime land surface temperatures in the summer. Here, we estimate that in 2024 wildfires between 1986 and 2023 in the Canadian boreal biome had an overall biome-wide annual warming effect with the land surface being 0.12 ± 0.04°C warmer during the daytime compared to a scenario without wildfire disturbance. About 40% (0.05°C) of the warming effect in 2023 is caused by the extreme wildfire season of 2023, which burned about 14,000,000 ha of the Canadian boreal forest. Burned area in 2023 was more than 700% larger than the mean burned area between 2001 and 2020. The annual warming effect resulted from the summertime (July–August) warming effect of 0.27 ± 0.09°C exceeding the wintertime (February–April) cooling effect of 0.02 ± 0.07°C (Figure 10). For a high burn area increase scenario of +150% between 2020 and 2050, the annual warming effect is estimated to increase to 0.16 ± 0.04°C by 2050 because of an increasing summertime warming effect. In contrast, a low burn area increase scenario of +36% between 2020 and 2050 results in no increase by 2050. It should be noted that these scenarios do not account for extreme fire years such as 2023 in the future.

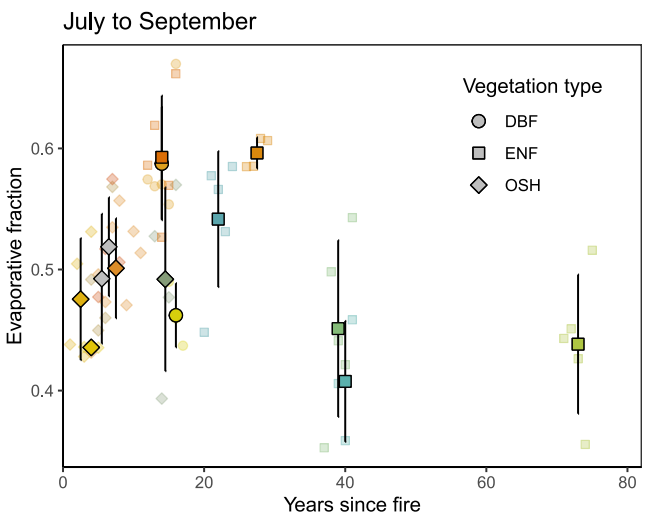

Figure 8. Successional trajectories of mean afternoon evaporative fraction during late summer. Solid circles show mean site averages. Symbols indicate vegetation type (DBF = deciduous broadleaf forest, ENF = evergreen needleleaf forest, OSH = open shrubland). Light colored circles show individual years. Gray colored symbols show sites with dominance of standing dead trees.

4. Discussion

In this study, we show that wildfire disturbance in the North American boreal biome exerts an overall warming effect on land surface temperatures with contrasting warming and cooling in the summer and winter, respectively. Previously, Rogers et al. (2013) reported an annual cooling effect caused by post-fire vegetation changes and increased albedo in the late winter months. They did not find substantial summer warming even though they simulated shorter post-fire roughness lengths and limited heating of the ground. In contrast, Amiro et al. (1999) detected daytime surface radiometric temperatures during the summer to be up to 6°C warmer in fire-affected areas of central Canada with warming effects being still evident after 15 years. Similar, findings were reported by Chambers and Chapin III (2003) for interior Alaska, where elevated surface temperatures and enhanced ground heat flux were observed during the first post-fire decade. Here, we show that

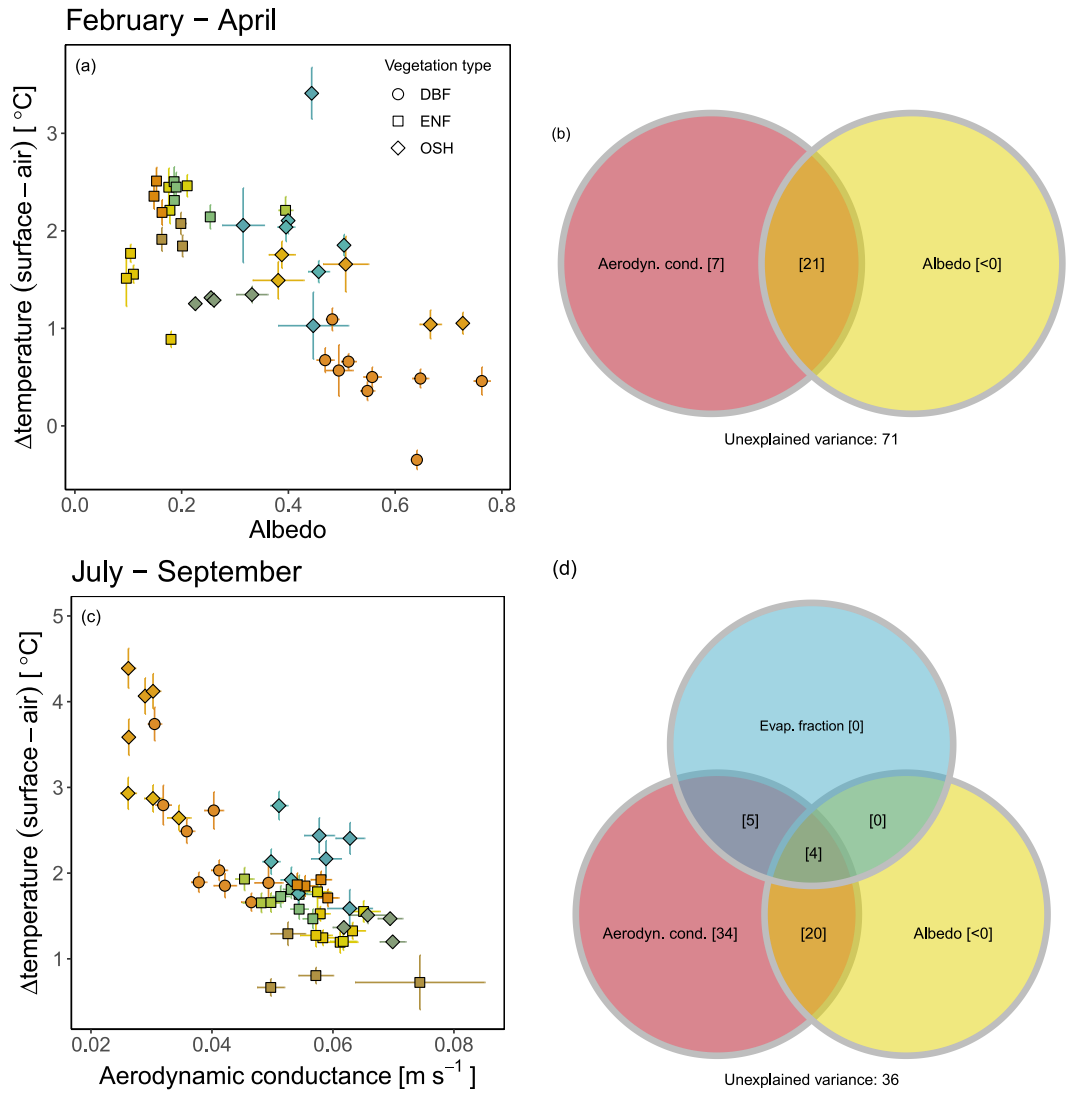

Figure 9. Relationship between mean afternoon surface-to-air temperature differences in the (a) winter and (c) summer and albedo and aerodynamic conductance, respectively. Percentage of variation in mean afternoon surface-to-air temperature differences explained by (b) aerodynamic conductance and albedo in the winter and (d) aerodynamic conductance, albedo, and evaporative fraction in the summer. The percentage of variance unexplained by any of the explanatory variables is shown at the bottom.

surface roughness changes with successional post-fire vegetation changes contribute substantially to the surface temperature effects, particularly during the summer. Changes to standing dead trees after a fire disturbance can have significant effects on land surface temperatures. However, structural changes related to standing dead trees are complex and remain difficult to predict (Aakala et al., 2008; Köster et al., 2016; Morrison & Raphael, 1993). Satellite-based LIDAR observations, such as through the Global Ecosystems Dynamics Investigation (GEDI) mission, can be leveraged to better understand drivers of changes in post-fire canopy heights (Folharini et al., 2022; Lang et al., 2023). Canopy height information can then be used to infer changes in post-fire vegetation roughness changes (Raupach, 1994).

Here, we did not investigate the effects of burn severity on land surface temperature impacts. Burn severity can affect land surface temperatures both through its effect on albedo and on successional pathways (e.g., changes in vegetation composition) (Jin et al., 2012; Wang et al., 2016). Additionally, boreal forest stands can follow multiple successional pathways as a result of varying edaphic conditions or neighborhood effects (Taylor & Chen, 2011). In this study, we sampled a wide range of wildfires across the North American boreal biome likely

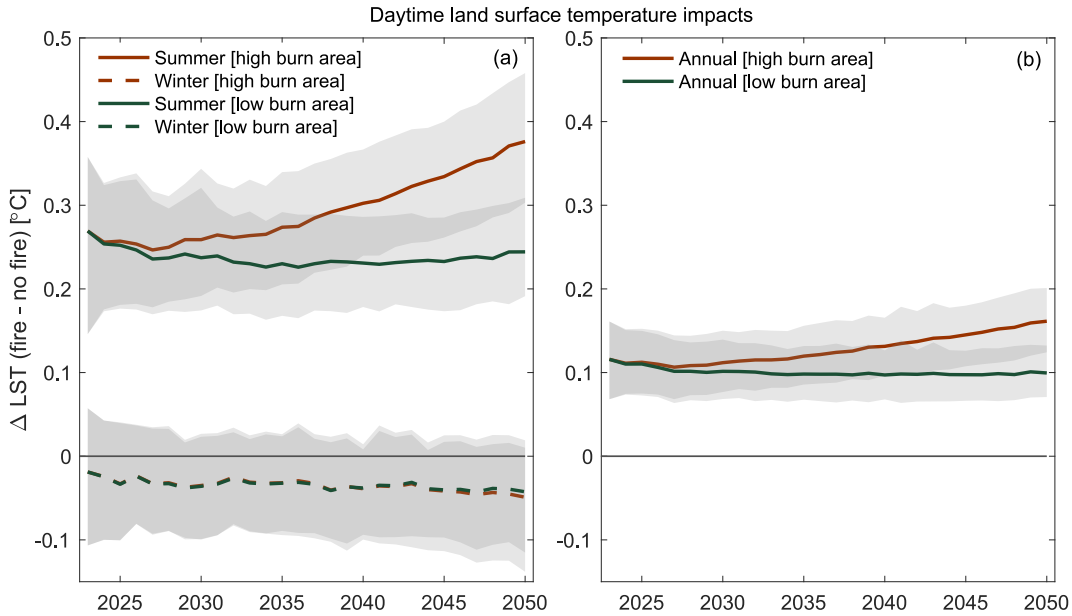

Figure 10. Estimated changes in summer- and wintertime daytime land surface temperatures caused by wildfire disturbance in the Canadian boreal biome (a) and in annual daytime land surface temperature (b) for the period 2024–2050. Results are shown for a high and low burn area increase scenario as reported by Phillips et al. (2022).

covering a wide range of burn severity and successional pathways. Remaining unexplained differences in post-fire land surface temperature effects might thus be partly caused by differences in burn severity and in environmental factors leading to multiple successional pathways.

Burned area and wildfire frequency is expected to increase over the next few decades (Hanes et al., 2019; Phillips et al., 2022). Thus, positive daytime surface temperature trends due to direct climate change effects are expected to accelerate with enhanced warming in burned areas. We found that, in 2024, the entire Canadian boreal biome was 0.12°C warmer than a biome lacking fire disturbance and that the warming impact is expected to increase by about a third for a high burn area increase scenario. In areas affected by permafrost, the accelerated surface warming likely will accelerate permafrost warming and eventually lead to disappearance (Holloway et al., 2020; Smith et al., 2022). Temperature acclimation of boreal evergreen species to warmer temperatures is more constrained for photosynthesis than for respiration (Crous et al., 2022) and soil respiration is expected to increase with warmer soil temperatures (Karhu et al., 2010) suggesting that accelerated fire-induced warming could reduce the carbon sink in the North American boreal forest. However, fire-induced changes in vegetation composition might be stronger leading to an enhanced boreal carbon sink (Mack et al., 2021).

Results from this study cannot be readily transferred to other forested biomes affected by wildfires such as temperate and tropical forests. Summer surface temperature impacts mainly depend on differences in evapotranspiration and forest structure between pre- and post-fire ecosystems. Shorter periods or absence of snow cover in temperate and tropical regions will substantially diminish or eliminate the winter cooling effect of wildfires (Webb et al., 2021). Additionally, in temperate and tropical forests, evaporative cooling is often stronger than in boreal forests (Liu et al., 2019), thus exceeding the influence of post-fire roughness changes on surface temperatures.

In a warming climate with changing boreal fire dynamics (Jones et al., 2022), it remains unclear if post-fire successional vegetation changes remain the same, potentially altering the integrated fire impacts on surface temperatures. For example, multiple and more frequent fire disturbances can alter successional pathways in favor of fire-adapted deciduous species (Anoszko et al., 2022; Johnstone & Chapin, 2006). Similarly, increased fire severity has been shown to lead to increasingly deciduous-dominated landscapes in Alaska (Johnstone et al., 2010). At the same time, climate change is expected to shorten the snow cover period, likely reducing the wintertime cooling effects of wildfires (Potter et al., 2020). Additionally, shortening of fire-return intervals could prevent post-fire return to mature boreal forests (Whitman et al., 2019) and prolong surface warming impacts

from reduced efficiency of heat transfer. Such changes in successional pathways and snow cover dynamics in a warming climate need to be further investigated to better understand the changing impacts of boreal wildfires on surface temperatures. Our study highlights the important daytime warming effect of boreal wildfires in North America on land surface temperatures. With increasingly larger areas experiencing wildfires more often, we can expect summertime daytime surface temperatures to increase more rapidly with far reaching consequences for ecological processes and ecosystem services.

Conflict of Interest

The authors declare no conflicts of interest relevant to this study.

Data Availability Statement

The R and Matlab codes for data processing, statistical analyses, and visualization and associated data sets are available at Zenodo via https://doi.org/10.5281/zenodo.13225460 (Helbig, 2024). All AmeriFlux data analyzed in this paper are publicly available via Amiro (2020a, 2020b, 2019), Goulden (2019a, 2019b, 2019c, 2019d, 2019e, 2019f), Randerson (2016a, 2016b), and Ueyama et al. (2023, 2024). MODIS satellite observations for study sites can be accessed through the Global Subsets Tool provided by ORNL DAAC (2018) (https://modis.ornl.gov/globalsubset/) and are available in Helbig (2024).

Acknowledgments
Funding for this study has been provided by the Natural Sciences and Engineering Research Council of Canada (NSERC) Discovery Grant program (RGPIN-02565-21) and the Arctic Challenge for Sustainability II (ArCS II; JPMXD1420318865). We acknowledge all data contributors that have openly shared their data sets through the AmeriFlux Network. We would also like to thank Brian Amiro for valuable comments on an earlier version of this manuscript. Open Access funding enabled and organized by Projekt DEAL.

References

Aakala, T., Kuuluvainen, T., Gauthier, S., & De Grandpré, L. (2008). Standing dead trees and their decay-class dynamics in the northeastern boreal old-growth forests of Quebec. *Forest Ecology and Management*, *255*(3–4), 410–420. https://doi.org/10.1016/j.foreco.2007.09.008

Amiro, B. D. (2019). AmeriFlux BASE CA-SF2 Saskatchewan—Western Boreal, forest burned in 1989, version 3-5, AmeriFlux AMP [Dataset]. https://doi.org/10.17190/AMF/1246007

Amiro, B. D. (2020a). AmeriFlux BASE CA-SF1 Saskatchewan—Western Boreal, forest burned in 1977, version 2-5, AmeriFlux AMP [Dataset]. https://doi.org/10.17190/AMF/1246006

Amiro, B. D. (2020b). AmeriFlux BASE CA-SF3 Saskatchewan—Western Boreal, forest burned in 1998, version 2-5, AmeriFlux AMP [Dataset]. https://doi.org/10.17190/AMF/1246008

Amiro, B. D., MacPherson, J. I., & Desjardins, R. L. (1999). BOREAS flight measurements of forest-fire effects on carbon dioxide and energy fluxes. *Agricultural and Forest Meteorology*, *96*, 199–208.

Amiro, B. D., Orchansky, A. L., Barr, A. G., Black, T. A., Chambers, S. D., Chapin, I. I. I. F. S., et al. (2006). The effect of post-fire stand age on the boreal forest energy balance. *Agricultural and Forest Meteorology*, *140*(1–4), 41–50. https://doi.org/10.1016/j.agrformet.2006.02.014

Amiro, B. D., Todd, J. B., Wotton, B. M., Logan, K. A., Flannigan, M. D., Stocks, B. J., et al. (2001). Direct carbon emissions from Canadian forest fires, 1959-1999. *Canadian Journal of Forest Research*, *31*(3), 512–525. https://doi.org/10.1139/x00-197

Anoszko, E., Frelich, L. E., Rich, R. L., & Reich, P. B. (2022). Wind and fire: Rapid shifts in tree community composition following multiple disturbances in the southern boreal forest. *Ecosphere*, *13*(3), e3952. https://doi.org/10.1002/ecs2.3952

Baldocchi, D., Kelliher, F. M., Black, T. A., & Jarvis, P. (2000). Climate and vegetation controls on boreal zone energy exchange. *Global Change Biology*, *6*(S1), 69–83. https://doi.org/10.1046/j.1365-2486.2000.06014.x

Balshi, M. S., McGUIRE, A. D., Duffy, P., Flannigan, M., Walsh, J., & Melillo, J. (2009). Assessing the response of area burned to changing climate in western boreal North America using a Multivariate Adaptive Regression Splines (MARS) approach. *Global Change Biology*, *15*(3), 578–600. https://doi.org/10.1111/j.1365-2486.2008.01679.x

Barker, C. A., Amiro, B. D., Kwon, H., Ewers, B. E., & Angstmann, J. L. (2009). Evapotranspiration in intermediate-aged and mature fens and upland black spruce boreal forests. *Ecohydrology*, *2*(4), 462–471. https://doi.org/10.1002/eco.74

Beck, P. S. A., Goetz, S. J., Mack, M. C., Alexander, H. D., Jin, Y., Randerson, J. T., & Loranty, M. M. (2011). The impacts and implications of an intensifying fire regime on Alaskan boreal forest composition and albedo. *Global Change Biology*, *17*(9), 2853–2866. https://doi.org/10.1111/j.1365-2486.2011.02412.x

Betts, R. A. (2000). Offset of the potential carbon sink from boreal forestation by decreases in surface albedo. *Nature*, *408*(6809), 187–190. https://doi.org/10.1038/35041545

Bonan, G. B. (2008). Forests and climate change: Forcings, feedbacks, and the climate benefits of forests. *Science*, *320*(5882), 1444–1449. https://doi.org/10.1126/science.1155121

Bond-Lamberty, B., Peckham, S. D., Ahl, D. E., & Gower, S. T. (2007). Fire as the dominant driver of central Canadian boreal forest carbon balance. *Nature*, *450*(7166), 89–92. https://doi.org/10.1038/nature06272

Bond-Lamberty, B., Peckham, S. D., Gower, S. T., & Ewers, B. E. (2009). Effects of fire on regional evapotranspiration in the central Canadian boreal forest. *Global Change Biology*, *15*(5), 1242–1254. https://doi.org/10.1111/j.1365-2486.2008.01776.x

Bond-Lamberty, B., Wang, C., Gower, S. T., & Norman, J. (2002). Leaf area dynamics of a boreal black spruce fire chronosequence. *Tree Physiology*, *22*(14), 993–1001. https://doi.org/10.1093/treephys/22.14.993

Brandt, J. P. (2009). The extent of the North American boreal zone. *Environmental Reviews*, *17*, 101–161. https://doi.org/10.1139/a09-004

Brandt, J. P., Flannigan, M. D., Maynard, D. G., Thompson, I. D., & Volney, W. J. A. (2013). An introduction to Canada's boreal zone: Ecosystem processes, health, sustainability, and environmental issues. *Environmental Reviews*, *21*(4), 207–226. https://doi.org/10.1139/er-2013-0040

Bronson, D. R., Gower, S. T., Tanner, M., Linder, S., & Van Herk, I. (2008). Response of soil surface CO_2 flux in a boreal forest to ecosystem warming. *Global Change Biology*, *14*(4), 856–867. https://doi.org/10.1111/j.1365-2486.2007.01508.x

Chambers, S. D., Beringer, J., Randerson, J. T., & Chapin, I. I. I. F. S. (2005). Fire effects on net radiation and energy partitioning: Contrasting responses of tundra and boreal forest ecosystems. *Journal of Geophysical Research*, *110*(D9), D09106. https://doi.org/10.1029/2004JD005299

Chambers, S. D., & Chapin, I. I. I. F. S. (2003). Fire effects on surface-atmosphere energy exchange in Alaskan black spruce ecosystems: Implications for feedbacks to regional climate. *Journal of Geophysical Research*, *107*(D1), FFR1-1–FFR1-17. https://doi.org/10.1029/2001jd000530

Cho, J., Miyazaki, S., Yeh, P. J.-F., Kim, W., Kanae, S., & Oki, T. (2011). Testing the hypothesis on the relationship between aerodynamic roughness length and albedo using vegetation structure parameters. *International Journal of Biometeorology*, *56*(2), 411–418. https://doi.org/10.1007/s00484-011-0445-2

Chu, H., & Hufkens, K. (2022). amerifluxr: Interface to "AmeriFlux" data services. Retrieved from https://cran.r-project.org/web/packages/amerifluxr/index.html

Crous, K. Y., Uddling, J., & De Kauwe, M. G. (2022). Temperature responses of photosynthesis and respiration in evergreen trees from boreal to tropical latitudes. *New Phytologist*, *234*(2), 353–374. https://doi.org/10.1111/nph.17951

Dawe, D. A., Parisien, M.-A., Van Dongen, A., & Whitman, E. (2022). Initial succession after wildfire in dry boreal forests of northwestern North America. *Plant Ecology*, *223*(7), 789–809. https://doi.org/10.1007/s11258-022-01237-6

de Groot, W. J., Flannigan, M. D., & Cantin, A. S. (2013). Climate change impacts on future boreal fire regimes. *Forest Ecology and Management*, *294*, 35–44. https://doi.org/10.1016/j.foreco.2012.09.027

Ebel, B. A., & Moody, J. A. (2017). Synthesis of soil-hydraulic properties and infiltration timescales in wildfire-affected soils. *Hydrological Processes*, *31*(2), 324–340. https://doi.org/10.1002/hyp.10998

Esseen, P.-A., Ehnström, B., Ericson, L., & Sjöberg, K. (1997). Boreal forests. *Ecological Bulletins*, *16–47*.

Folharini, S., dos Santos, S. M. B., Bento-Gonçalves, A., & Vieira, A. (2022). Estimation of tree height in burned areas with GEDI laser data in northern Portugal and Galicia (Spain). *Environmental Sciences Proceedings*, *22*, 50.

Gibson, C. M., Chasmer, L. E., Thompson, D. K., Quinton, W. L., Flannigan, M. D., & Olefeldt, D. (2018). Wildfire as a major driver of recent permafrost thaw in boreal peatlands. *Nature Communications*, *9*(1), 3041. https://doi.org/10.1038/s41467-018-05457-1

Gleason, K. E., McConnell, J. R., Arienzo, M. M., Chellman, N., & Calvin, W. M. (2019). Four-fold increase in solar forcing on snow in western U.S. burned forests since 1999. *Nature Communications*, *10*(1), 2026. https://doi.org/10.1038/s41467-019-09935-y

Goulden, M. (2019a). AmeriFlux BASE CA-NS2 UCI-1930 burn site, version 3-5, AmeriFlux AMP [Dataset]. https://doi.org/10.17190/AMF/1245999

Goulden, M. (2019b). AmeriFlux BASE CA-NS3 UCI-1964 burn site, version 3-5, AmeriFlux AMP [Dataset]. https://doi.org/10.17190/AMF/1246000

Goulden, M. (2019c). AmeriFlux BASE CA-NS4 UCI-1964 burn site wet, Version 3-5, AmeriFlux AMP [Dataset]. https://doi.org/10.17190/AMF/1246001

Goulden, M. (2019d). AmeriFlux BASE CA-NS5 UCI-1981 burn site, version 3-5, AmeriFlux AMP [Dataset]. https://doi.org/10.17190/AMF/1246002

Goulden, M. (2019e). AmeriFlux BASE CA-NS6 UCI-1989 burn site, version 3-5, AmeriFlux AMP [Dataset]. https://doi.org/10.17190/AMF/1246003

Goulden, M. (2019f). AmeriFlux BASE CA-NS7 UCI-1998 burn site, version 3-5, AmeriFlux AMP [Dataset]. https://doi.org/10.17190/AMF/1246004

Halim, M. A., Chen, H. Y. H., & Thomas, S. C. (2019). Stand age and species composition effects on surface albedo in a mixedwood boreal forest. *Biogeosciences*, *16*(22), 4357–4375. https://doi.org/10.5194/bg-16-4357-2019

Hampton, T. B., & Basu, N. B. (2022). A novel Budyko-based approach to quantify post-forest-fire streamflow response and recovery timescales. *Journal of Hydrology*, *608*, 127685. https://doi.org/10.1016/j.jhydrol.2022.127685

Hanes, C. C., Wang, X., Jain, P., Parisien, M.-A., Little, J. M., & Flannigan, M. D. (2019). Fire-regime changes in Canada over the last half century. *Canadian Journal of Forest Research*, *49*(3), 256–269. https://doi.org/10.1139/cjfr-2018-0293

Hansen, M. C., Potapov, P. V., Moore, R., Hancher, M., Turubanova, S. A., Tyukavina, A., et al. (2013). High-resolution global maps of 21st-century forest cover change. *Science*, *342*(6160), 850–853. https://doi.org/10.1126/science.1244693

Harden, J. W., Trumbore, S. E., Stocks, B. J., Hirsch, A., Gower, S. T., O'neill, K. P., & Kasischke, E. S. (2000). The role of fire in the boreal carbon budget. *Global Change Biology*, *6*(S1), 174–184. https://doi.org/10.1046/j.1365-2486.2000.06019.x

Helbig, M. (2024). Boreal wildfire v1.0.0 [Software and Dataset]. *Zenodo*. https://doi.org/10.5281/zenodo.13225460

Helbig, M., Waddington, J. M., Alekseychik, P., Amiro, B., Aurela, M., Barr, A. G., et al. (2020). The biophysical climate mitigation potential of boreal peatlands during the growing season. *Environmental Research Letters*, *15*(10), 104004. https://doi.org/10.1088/1748-9326/abab34

Holloway, J. E., Lewkowicz, A. G., Douglas, T. A., Li, X., Turetsky, M. R., Baltzer, J. L., & Jin, H. (2020). Impact of wildfire on permafrost landscapes: A review of recent advances and future prospects. *Permafrost and Periglacial Processes*, *31*(3), 371–382. https://doi.org/10.1002/ppp.2048

Hulley, G. (2021). MODIS/Aqua land surface temperature/3-band emissivity 8-day L3 global 1km SIN grid V061. Retrieved from https://lpdaac.usgs.gov/products/myd21a2v061/

Hulley, G., & Hook, S. (2017). MOD21A2 MODIS/Terra land surface temperature/3-band emissivity 8-day L3 global 1km SIN grid V006. Retrieved from https://lpdaac.usgs.gov/products/mod21a2v006/

Jiang, Y., Rocha, A. V., O'Donnell, J. A., Drysdale, J. A., Rastetter, E. B., Shaver, G. R., & Zhuang, Q. (2015). Contrasting soil thermal responses to fire in Alaskan tundra and boreal forest. *Journal of Geophysical Research: Earth Surface*, *120*(2), 363–378. https://doi.org/10.1002/2014jf003180

Jin, Y., Randerson, J. T., Goetz, S. J., Beck, P. S. A., Loranty, M. M., & Goulden, M. L. (2012). The influence of burn severity on postfire vegetation recovery and albedo change during early succession in North American boreal forests. *Journal of Geophysical Research*, *117*(G1), G01036. https://doi.org/10.1029/2011JG001886

Johnstone, J. F., & Chapin, F. S. (2006). Fire interval effects on successional trajectory in boreal forests of northwest Canada. *Ecosystems*, *9*(2), 268–277. https://doi.org/10.1007/s10021-005-0061-2

Johnstone, J. F., Hollingsworth, T. N., Chapin Iii, F. S., & Mack, M. C. (2010). Changes in fire regime break the legacy lock on successional trajectories in Alaskan boreal forest. *Global Change Biology*, *16*(4), 1281–1295. https://doi.org/10.1111/j.1365-2486.2009.02051.x

Jones, M. W., Abatzoglou, J. T., Veraverbeke, S., Andela, N., Lasslop, G., Forkel, M., et al. (2022). Global and regional trends and drivers of fire under climate change. *Reviews of Geophysics*, *60*(3), e2020RG000726. https://doi.org/10.1029/2020rg000726

Kang, S., Kimball, J. S., & Running, S. W. (2006). Simulating effects of fire disturbance and climate change on boreal forest productivity and evapotranspiration. *Science of the Total Environment*, *362*(1–3), 85–102. https://doi.org/10.1016/j.scitotenv.2005.11.014

Karhu, K., Fritze, H., Hämäläinen, K., Vanhala, P., Jungner, H., Oinonen, M., et al. (2010). Temperature sensitivity of soil carbon fractions in boreal forest soil. *Ecology*, *91*(2), 370–376. https://doi.org/10.1890/09-0478.1

Kasischke, E. S., & Turetsky, M. R. (2006). Recent changes in the fire regime across the North American boreal region—Spatial and temporal patterns of burning across Canada and Alaska. *Geophysical Research Letters*, *33*(9). L09703. https://doi.org/10.1029/2006GL025677

Keenan, R. J., Reams, G. A., Achard, F., de Freitas, J. V., Grainger, A., & Lindquist, E. (2015). Dynamics of global forest area: Results from the FAO global forest resources assessment 2015. *Forest Ecology and Management*, *352*, 9–20. https://doi.org/10.1016/j.foreco.2015.06.014

Kelly, R., Chipman, M. L., Higuera, P. E., Stefanova, I., Brubaker, L. B., & Hu, F. S. (2013). Recent burning of boreal forests exceeds fire regime limits of the past 10,000 years. *Proceedings of the National Academy of Sciences of the United States of America*, *110*(32), 13055–13060. https://doi.org/10.1073/pnas.1305069110

Knauer, J., Wutzler, T., Bennett, A., Zaehle, S., El-Madany, T., & Migliavacca, M. (2022). bigleaf: Physical and physiological ecosystem properties from eddy covariance data. Retrieved from https://cran.r-project.org/web/packages/bigleaf/index.html

Köster, K., Köster, E., Orumaa, A., Parro, K., Jõgiste, K., Berninger, F., et al. (2016). How time since forest fire affects stand structure, soil physical-chemical properties and soil CO_2 efflux in hemiboreal scots pine forest fire chronosequence? *Forests*, *7*(9), 201. https://doi.org/10.3390/f7090201

Lang, N., Jetz, W., Schindler, K., & Wegner, J. D. (2023). A high-resolution canopy height model of the Earth. *Nature Ecology & Evolution*, *7*(11), 1778–1789. https://doi.org/10.1038/s41559-023-02206-6

Leuning, R., Zhang, Y. Q., Rajaud, A., Cleugh, H., & Tu, K. (2008). A simple surface conductance model to estimate regional evaporation using MODIS leaf area index and the Penman-Monteith equation. *Water Resources Research*, *44*(10), W10419. https://doi.org/10.1029/2007WR006562

Liao, W., Rigden, A. J., & Li, D. (2018). Attribution of local temperature response to deforestation. *Journal of Geophysical Research: Biogeosciences*, *123*(5), 1572–1587. https://doi.org/10.1029/2018jg004401

Lindroth, A. (1993). Aerodynamic and canopy resistance of short-rotation forest in relation to leaf area index and climate. *Boundary-Layer Meteorology*, *66*(3), 265–279. https://doi.org/10.1007/bf00705478

Liu, H., & Randerson, J. T. (2008). Interannual variability of surface energy exchange depends on stand age in a boreal forest fire chronosequence. *Journal of Geophysical Research*, *113*(G1), G01006. https://doi.org/10.1029/2007JG000483

Liu, H., Randerson, J. T., Lindfors, J., & Chapin, I. I. I. F. S. (2005). Changes in the surface energy budget after fire in boreal ecosystems of interior Alaska: An annual perspective. *Journal of Geophysical Research*, *110*(D13), D13101. https://doi.org/10.1029/2004JD005158

Liu, Z., Ballantyne, A. P., & Cooper, L. A. (2018). Increases in land surface temperature in response to fire in Siberian boreal forests and their attribution to biophysical processes. *Geophysical Research Letters*, *45*(13), 6485–6494. https://doi.org/10.1029/2018gl078283

Liu, Z., Ballantyne, A. P., & Cooper, L. A. (2019). Biophysical feedback of global forest fires on surface temperature. *Nature Communications*, *10*(1), 214. https://doi.org/10.1038/s41467-018-08237-z

Lloyd, J., & Taylor, J. A. (1994). On the temperature dependence of soil respiration. *Functional Ecology*, *8*(3), 315–323. https://doi.org/10.2307/2389824

Lyons, E. A., Jin, Y., & Randerson, J. T. (2008). Changes in surface albedo after fire in boreal forest ecosystems of interior Alaska assessed using MODIS satellite observations. *Journal of Geophysical Research*, *113*(G2), G02012. https://doi.org/10.1029/2007JG000606

Mack, M. C., Walker, X. J., Johnstone, J. F., Alexander, H. D., Melvin, A. M., Jean, M., & Miller, S. N. (2021). Carbon loss from boreal forest wildfires offset by increased dominance of deciduous trees. *Science*, *372*(6539), 280–283. https://doi.org/10.1126/science.abf3903

Mahrt, L., Sun, J., MacPherson, J. I., Jensen, N. O., & Desjardins, R. L. (1997). Formulation of surface heat flux: Application to BOREAS. *Journal of Geophysical Research*, *102*(D24), 29641–29649. https://doi.org/10.1029/97jd01116

Morrison, M. L., & Raphael, M. G. (1993). Modeling the dynamics of snags. *Ecological Applications*, *3*(2), 322–330. https://doi.org/10.2307/1941835

Myneni, R., Knyazikhin, Y., & Park, T. (2015). MOD15A2H MODIS/Terra leaf area index/FPAR 8-day L4 global 500m SIN grid V006. Retrieved from https://lpdaac.usgs.gov/products/mod15a2hv006/

Nakai, T., Sumida, A., Daikoku, K., Matsumoto, K., van der Molen, M. K., Kodama, Y., et al. (2008). Parameterisation of aerodynamic roughness over boreal, cool- and warm-temperate forests. *Agricultural and Forest Meteorology*, *148*(12), 1916–1925. https://doi.org/10.1016/j.agrformet.2008.03.009

Natural Resources Canada. (2020). Land cover of Canada—Open government portal. Retrieved from https://open.canada.ca/data/en/dataset/ee1580ab-a23d-4f86-a09b-79763677eb47

Nolan, R. H., Collins, L., Leigh, A., Ooi, M. K. J., Curran, T. J., Fairman, T. A., et al. (2021). Limits to post-fire vegetation recovery under climate change. *Plant, Cell and Environment*, *44*(11), 3471–3489. https://doi.org/10.1111/pce.14176

Novick, K. A., & Katul, G. G. (2020). The duality of reforestation impacts on surface and air temperature. *Journal of Geophysical Research: Biogeosciences*, *125*(4), e2019JG005543. https://doi.org/10.1029/2019jg005543

Oksanen, J., Simpson, G. L., Blanchet, F. G., Kindt, R., Legendre, P., Minchin, P. R., et al. (2024). vegan: Community ecology package. Retrieved from https://cran.r-project.org/web/packages/vegan/index.html

O'Leary, I. I. I. D., Hall, D. K., Medler, M., Matthews, R., & Flower, A. (2001-2018). 2020 snowmelt timing maps derived from MODIS for North America, version 2. *ORNL DAAC*. Retrieved from https://daac.ornl.gov/cgi-bin/dsviewer.pl?ds_id=1712

ORNL DAAC. (2018). Terrestrial ecology subsetting & visualization services (TESViS) global subset tool [Software]. *ORNL DAAC*. https://doi.org/10.3334/ORNLDAAC/1379

Panwar, A., Renner, M., & Kleidon, A. (2020). Imprints of evaporative conditions and vegetation type in diurnal temperature variations. *Hydrology and Earth System Sciences*, *24*(10), 4923–4942. https://doi.org/10.5194/hess-24-4923-2020

Phillips, C. A., Rogers, B. M., Elder, M., Cooperdock, S., Moubarak, M., Randerson, J. T., & Frumhoff, P. C. (2022). Escalating carbon emissions from North American boreal forest wildfires and the climate mitigation potential of fire management. *Science Advances*, *8*(17), eabl7161. https://doi.org/10.1126/sciadv.abl7161

Pimentel, R., & Arheimer, B. (2021). Hydrological impacts of a wildfire in a Boreal region: The Västmanland fire 2014 (Sweden). *Science of the Total Environment*, *756*, 143519. https://doi.org/10.1016/j.scitotenv.2020.143519

Potter, S., Solvik, K., Erb, A., Goetz, S. J., Johnstone, J. F., Mack, M. C., et al. (2020). Climate change decreases the cooling effect from postfire albedo in boreal North America. *Global Change Biology*, *26*(3), 1592–1607. https://doi.org/10.1111/gcb.14888

Qian, Y., Gustafson, W. I., Jr., Leung, L. R., & Ghan, S. J. (2009). Effects of soot-induced snow albedo change on snowpack and hydrological cycle in western United States based on Weather Research and Forecasting chemistry and regional climate simulations. *Journal of Geophysical Research*, *114*, D03108. https://doi.org/10.1029/2008jd011039

Randerson, J. T. (2016a). AmeriFlux BASE US-Bn2 Bonanza Creek, 1987 burn site near delta junction, version 1-1 [Dataset]. *AmeriFlux AMP*. https://doi.org/10.17190/AMF/1246034

Randerson, J. T. (2016b). AmeriFlux BASE US-Bn3 Bonanza Creek, 1999 burn site near delta junction, version 1-1 [Dataset]. *AmeriFlux AMP*. https://doi.org/10.17190/AMF/1246035

Randerson, J. T., Liu, H., Flanner, M. G., Chambers, S. D., Jin, Y., Hess, P. G., et al. (2006). The impact of boreal forest fire on climate warming. *Science*, *314*(5802), 1130–1132. https://doi.org/10.1126/science.1132075

Raupach, M. R. (1994). Simplified expressions for vegetation roughness length and zero-plane displacement as functions of canopy height and area index. *Boundary-Layer Meteorology*, *71*(1–2), 211–216. https://doi.org/10.1007/bf00709229

Rogers, B. M., Randerson, J. T., & Bonan, G. B. (2013). High-latitude cooling associated with landscape changes from North American boreal forest fires. *Biogeosciences*, *10*(2), 699–718. https://doi.org/10.5194/bg-10-699-2013

Schaaf, C., & Wang, Z. (2021). MODIS/Terra+Aqua BRDF/Albedo daily L3 global—500m V061. Retrieved from https://lpdaac.usgs.gov/products/mcd43a3v061/

Skakun, R., Whitman, E., Little, J. M., & Parisien, M.-A. (2021). Area burned adjustments to historical wildland fires in Canada. *Environmental Research Letters*, *16*(6), 064014. https://doi.org/10.1088/1748-9326/abfb2c

Smith, S. L., O'Neill, H. B., Isaksen, K., Noetzli, J., & Romanovsky, V. E. (2022). The changing thermal state of permafrost. *Nature Reviews Earth & Environment*, *3*(1), 10–23. https://doi.org/10.1038/s43017-021-00240-1

Stralberg, D., Wang, X., Parisien, M.-A., Robinne, F.-N., Sólymos, P., Mahon, C. L., et al. (2018). Wildfire-mediated vegetation change in boreal forests of Alberta, Canada. *Ecosphere*, *9*(3), e02156. https://doi.org/10.1002/ecs2.2156

Taylor, A. R., & Chen, H. Y. H. (2011). Multiple successional pathways of boreal forest stands in central Canada. *Ecography*, *34*(2), 208–219. https://doi.org/10.1111/j.1600-0587.2010.06455.x

Thom, A. S. (1972). Momentum, mass and heat exchange of vegetation. *Quarterly Journal of the Royal Meteorological Society*, *98*(415), 124–134. https://doi.org/10.1256/smsqj.41509

Tsuyuzaki, S., Kushida, K., & Kodama, Y. (2009). Recovery of surface albedo and plant cover after wildfire in a Picea mariana forest in interior Alaska. *Climate Change*, *93*(3–4), 517–525. https://doi.org/10.1007/s10584-008-9505-y

Ueyama, M., Iwata, H., & Harazono, Y. (2023). AmeriFlux BASE US-Fcr Cascaden Ridge Fire Scar, version 3-5 [Dataset]. *AmeriFlux AMP*. https://doi.org/10.17190/AMF/1562388

Ueyama, M., Iwata, H., & Harazono, Y. (2024). AmeriFlux BASE US-Rpf Poker Flat Research Range: Succession from fire scar to deciduous forest, version 10-5. [Dataset]. *AmeriFlux AMP*. https://doi.org/10.17190/AMF/1579540

Ueyama, M., Yamamori, T., Iwata, H., & Harazono, Y. (2020). Cooling and moistening of the planetary boundary layer in interior Alaska due to a postfire change in surface energy exchange. *Journal of Geophysical Research: Atmospheres*, *125*(18), e2020JD032968. https://doi.org/10.1029/2020jd032968

USGS. (2016). NLCD 2016 land cover (Alaska)|multi-resolution land characteristics (MRLC) consortium. Retrieved from https://www.mrlc.gov/data/nlcd-2016-land-cover-alaska

Veraverbeke, S., Rogers, B. M., Goulden, M. L., Jandt, R. R., Miller, C. E., Wiggins, E. B., & Randerson, J. T. (2017). Lightning as a major driver of recent large fire years in North American boreal forests. *Nature Climate Change*, *7*, 529–534. https://doi.org/10.1038/nclimate3329

Walker, X. J., Baltzer, J. L., Cumming, S. G., Day, N. J., Ebert, C., Goetz, S., et al. (2019). Increasing wildfires threaten historic carbon sink of boreal forest soils. *Nature*, *572*(7770), 520–523. https://doi.org/10.1038/s41586-019-1474-y

Walker, X. J., Rogers, B. M., Baltzer, J. L., Cumming, S. G., Day, N. J., Goetz, S. J., et al. (2018). Cross-scale controls on carbon emissions from boreal forest megafires. *Global Change Biology*, *24*(9), 4251–4265. https://doi.org/10.1111/gcb.14287

Wang, Z., Erb, A. M., Schaaf, C. B., Sun, Q., Liu, Y., Yang, Y., et al. (2016). Early spring post-fire snow albedo dynamics in high latitude boreal forests using Landsat-8 OLI data. *Remote Sensing of Environment*, *185*, 71–83. https://doi.org/10.1016/j.rse.2016.02.059

Webb, E. E., Loranty, M. M., & Lichstein, J. W. (2021). Surface water, vegetation, and fire as drivers of the terrestrial Arctic-boreal albedo feedback. *Environmental Research Letters*, *16*(8), 084046. https://doi.org/10.1088/1748-9326/ac14ea

Whitman, E., Parisien, M.-A., Thompson, D. K., & Flannigan, M. D. (2019). Short-interval wildfire and drought overwhelm boreal forest resilience. *Scientific Reports*, *9*(1), 18796. https://doi.org/10.1038/s41598-019-55036-7

Yoshikawa, K., Bolton, W. R., Romanovsky, V. E., Fukuda, M., & Hinzman, L. D. (2002). Impacts of wildfire on the permafrost in the boreal forests of Interior Alaska. *Journal of Geophysical Research*, *107*(D1), FFR4-1–FFR4-14. https://doi.org/10.1029/2001jd000438

Zhao, J., Wang, L., Hou, X., Li, G., Tian, Q., Chan, E., et al. (2021). Fire regime impacts on postfire diurnal land surface temperature change over North American boreal forest. *Journal of Geophysical Research: Atmospheres*, *126*(23), e2021JD035589. https://doi.org/10.1029/2021jd035589